

Effect of Different sp^2 Bond Contents on the Reactivity and Mechanical Properties of Coke Carbon: A ReaxFF Molecular Dynamics Study

Zixin Xiong, Kejiang Li,* Yushan Bu, Zeng Liang, Hang Zhang, Haotian Liao, Feng Zhou, and Jianliang Zhang



Cite This: *ACS Omega* 2023, 8, 37043–37053



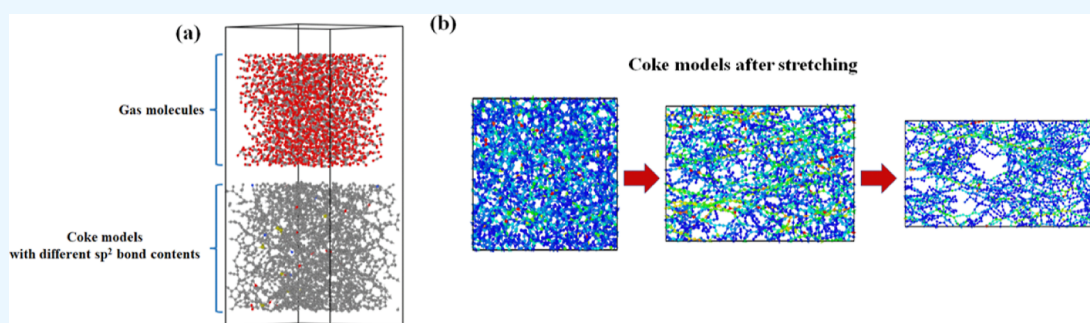
Read Online

ACCESS |

Metrics & More

Article Recommendations

Supporting Information



ABSTRACT: In this study, ReaxFF-MD was used to construct a large-molecule model of coke containing 3000 atoms, and the sp^2 bond content of the model was controlled by changing the heating and cooling rates. The increase of the sp^2 bond content led to a significant difference in the reactivity of coke. The presence of the sp^2 bond caused the carbon atoms inside the coke to change into a circular structure, making it more difficult for the gaseous atoms to adsorb on the surface of the coke. It significantly reduced the gasification reaction rate of coke in the CO_2 and H_2O atmospheres. In the tensile simulation experiment, it was found that the stretching process of coke was mainly divided into three stages: an elastic stretching stage, a plastic stretching stage, and a model fracture stage. During the stretching process, the carbon ring structure would undergo a C–C bond fracture while generating carbon chains to resist stress. The results indicated that the presence of sp^2 bonds can effectively reduce the phenomenon of excessive local stress on coke to improve its tensile resistance. The method developed in this paper may provide further ideas and platforms for the research on coke performance.

1. INTRODUCTION

As a reactive substance with both reducibility and high strength, coke remains one of the most important raw materials in the metallurgical production industry worldwide.^{1–4} Coke provides both heat for the ironmaking process and structural support for the melting zone of the blast furnace. The physical strength of coke is one of the important factors for the stable operation of blast furnaces.^{5–8} Zhang et al. found that high reactivity of the coke matrix and small pore size of coke can effectively avoid the erosion of coke by gasification.⁹ Pang et al. also found the influence of the pore structure and microstructure on the mechanical properties of coke through orthogonal gasification experiments.¹⁰ In blast furnace reactions, coke generally undergoes physical collisions and dissolution reactions.^{11–14} These situations will lead to a decrease in the strength of coke, thereby affecting its load support function in the ironmaking process. For the ironmaking industry, a deep understanding of the factors that affect coke strength is of great significance for its effective utilization.

The current experimental results indicated that the reaction performance and mechanical properties of coke mainly depend on its internal structure.^{15–18} In experimental research, X-ray diffraction (XRD) or scanning electronic microscopy methods are often used to observe the internal pore size distribution and microstructure.^{19–23} Lu et al.²⁴ confirmed that graphitized carbon indicates the main presence of carbon atoms in coke through X-ray photoelectron spectroscopy, which has a certain impact on the thermal properties of coke. Moreover, Sato et al. analyzed and estimated the tensile stress of coke cracking in coke ovens, and the results showed that coke can withstand tensile stress up to 10–20 MPa.²⁵ The above results provide a data

Received: June 21, 2023

Accepted: September 5, 2023

Published: September 27, 2023



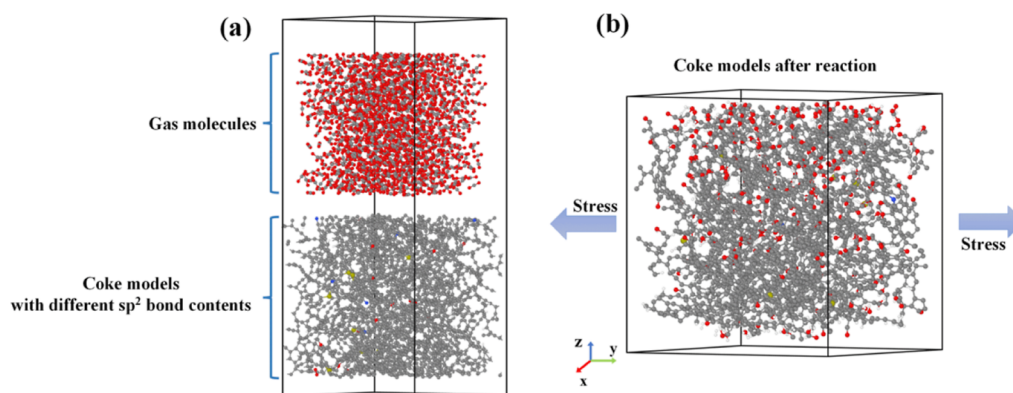


Figure 1. Simulation model: (a) coke reaction with different sp^2 bond contents; and (b) stretching model of the coke model, and the stretching direction is the y -direction.

reference for the simulation results. However, the content of sp^2 bonds may also be a key factor affecting the performance of coke. Zi-Zhao et al. used experimental methods such as XRD to characterize the carbon structure and found that as the graphitization degree increased, the strength of coke residue significantly decreased.²⁶ It indicates that the sp^2 bond content has a significant impact on the structure of coke in the experiments.

At present, the main methods for studying the performance and internal structure of coke are to simulate coke behavior by experiment. However, these methods cannot provide the microstructure evolution process of coke to explain its reaction mechanism. In order to gain a deeper understanding of the structural changes of carbon-containing materials during the reaction process, simulation methods using reactive force field (ReaxFF) and molecular dynamics (MD) have been widely used.^{27–31} These methods have been proven to be effective in studying the microstructural changes of carbon-containing materials under high-temperature conditions. Tian et al. used ReaxFF-MD to build a large coke molecular structure containing more than 60,000 atoms.³² This study found that the stacking structure and some chemical bonds such as sp^2 bonds played a key role in resisting external forces when the coke model was stressed. The role of the sp^2 bond was only qualitatively analyzed in this study, and no relevant exploration was conducted on the impact of its content. This study focused on the influence of different sp^2 bond contents on the structure of coke to gain a deeper understanding of the process of the microstructure changes.

This study investigated the effect of the sp^2 bond content on the reaction performance and mechanical properties of the coke configuration through ReaxFF-MD simulation. By constructing three different types of coke models with different sp^2 bond contents and conducting gasification reaction simulation and tensile simulation on the models, the influence of sp^2 bonds on the performance of coke and the mechanism of changes in the internal microstructure of coke are explored. This study can provide new ideas and methods for future research on the performance of coke.

2. SIMULATION METHODS

2.1. Construction of Coke Models at Different Degrees of Graphitization.

A coke model (molecular formula $C_{2863}H_{105}O_6N_{18}S_8$) was constructed in subsequent MD simulations to perform molecular dynamics simulations of the coke stretching process. This model has the same atomic ratio as

the molecular model of Pingyao coke used in Tian's article,³² which has been proven to simulate the reaction behavior of coke effectively. Previous studies have investigated the effects of density and time step on the structure and reaction performance of amorphous coke models.^{26,27,33}

The entire generation process of the coke model was carried out in the following four steps: (1) at the initial stage, the atoms were randomly generated inside the box by using the LAMMPS software package,³⁴ and the size of the box was determined by the model density and the total number of atoms. Li et al. have applied the force field parameters used in this study to the amorphous carbon model, while the density is 1.4 g/cm^3 and the time step is 0.2 fs .²⁷ We decided to set the time step and density in this study simulation to be consistent with Li's article after repeating some simulations and validation experiments. (2) The model was operated in the NVT ensemble at 300 K (room temperature) for 10 ps to eliminate floating bonds and minimize the total energy. (3) The third step was the heating stage, where the model was heated from 300 K to $4000 \text{ K}/5000 \text{ K}/6000 \text{ K}$ in 10 ps and was operated in the NVT ensemble at this temperature for 500 ps . (4) The final step was the cooling step. After repeated simulations, different cooling times have an impact on the sp^2 bond content of the coke model. In order to control the sp^2 bond content at a specific level, the cooling time was set to 10 and 20 ps . The model was cooled from the heating temperature to room temperature 300 K within different times (10 and 20 ps) and was operated in the NVT ensemble at 300 K for 500 ps .

In order to change the sp^2 bond content of the coke model, many related simulation attempts have been made to determine that the factors affecting the sp^2 bond content of the generated coke model are the final temperature of heating, the heating rate, and the cooling rate. By changing these three factors, the sp^2 bond content of the generated coke model can be effectively controlled. The specific simulation attempt data can be found in the [Supporting Information](#).

2.2. Simulations of the Coke Dissolution Reaction and Mechanical Properties.

The coke dissolution reaction process under different CO_2 and H_2O atmospheres was investigated using the coke model constructed above, and the specific reaction model is shown in [Figure 1a](#). The composition ratio of the atmosphere was changed to three situations: 1000 CO_2 molecules, 500 CO_2 molecules with $500\text{H}_2\text{O}$ molecules, and $1000\text{H}_2\text{O}$ molecules. Periodic boundaries were set in the x and y directions of the model, which was to enable the gas molecules to fully react with the coke model. Nonperiodic boundaries were set in the Z direction, allowing the gas

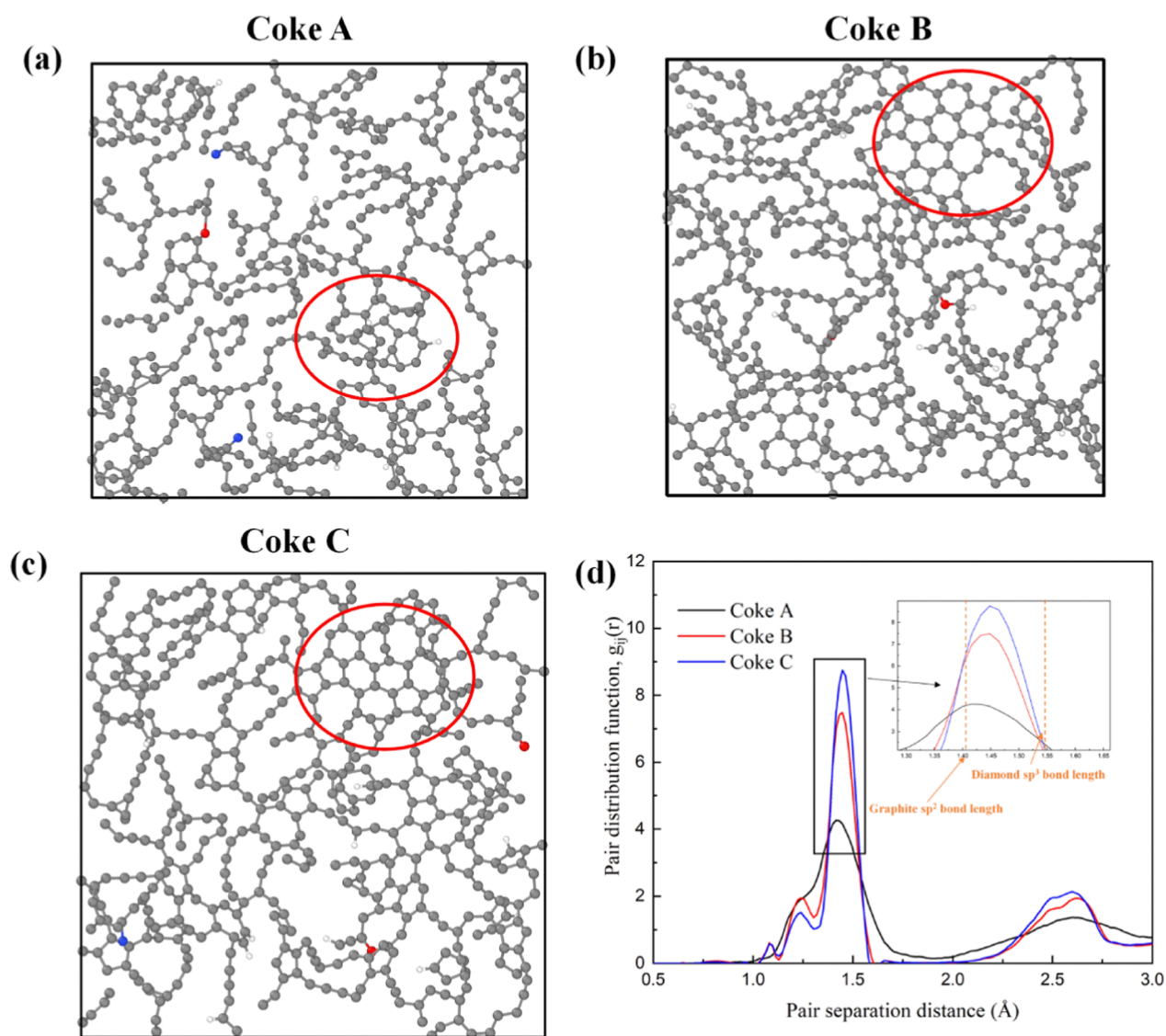


Figure 2. Front view of three types of coke models: (a) coke A; (b) coke B; and (c) coke C and (d) their responding pair distribution functions.

molecules to penetrate and react downward from the upper part of the coke model. The ReaxFF parameter was originally used in Plimpton's study,³⁴ and it has been validated for its feasibility in computing reaction paths, kinetics, transition states, and process energies.^{28,35,36} Moreover, this set of ReaxFF parameters was consistent with Li's research, which has been proved to better simulate the relevant gasification reaction of the carbon-containing models.^{27,37,38} In the process of the reaction, simulations of the coke model and gas molecules were performed in the *NPT* ensemble for 20 ps, which served to eliminate the unstable dangling bonds in the model and minimize the energy of the model. After that, the whole system was heated to 3500 K and was performed in the *NVT* ensemble for 1000 ps at 3500 K, allowing the coke model to fully react with gas molecules. Finally, the temperature of the whole system was reduced to 300 K.

To investigate the effect of the sp^2 bond content on the mechanical properties of coke, tensile experiments were conducted on both the unreacted model and the model after the solution loss reaction. They were conducted in the *NPT* ensemble, with a time step set to 0.1 fs in the simulation. Before stretching began, the system was relaxed at 300 K for 20 ps to

achieve equilibrium. Then, under the *NPT* ensemble, the model was relaxed at the target temperature for 20 ps. The relaxed coke model underwent uniaxial tension at a strain rate of 10^{-5} /ps along the *y*-axis direction, as shown in Figure 1b. The maximum strain was controlled at 80%, and at this stage, the structure of the coke model was completely fractured. The strain rate was determined based on research and tests.^{30,39–41} The stresses of all atoms were summed to get the total structural stress, and a stress–strain curve was plotted. For the convenience of statistical analysis, a Python program was conducted to distinguish and statistically analyze the lengths of different chemical bonds between atoms by using the function block of OVITO software to detect the bond length between atoms.⁴² This study focused on the changes in the coke models' structures during the stretching process and the mechanical properties of the coke model after different reaction conditions.

3. RESULTS AND DISCUSSION

3.1. Construction of Coke Models with Different sp^2 Bond Contents. Before starting the simulation, the conclusion that the use of amorphous carbon models can effectively reduce the reaction performance and mechanical properties of coke has

been drawn from the relevant research of Tian et al.³² In addition, a similar method has been adopted in this study to construct three coke models consisting of 3000 atoms at different temperatures. However, the sp^2 bond content in the coke model constructed in this way is not fixed, which has a certain impact on the performance of the coke models. To change the content of sp^2 bonds, three coke models were constructed with different sp^2 bond contents by changing the heating and cooling rates during the model construction process. The specific simulation attempt process is shown in the Supporting Information. As shown in (Figure 2a–c), there are section screenshots of three models with different sp^2 bond contents. With the increase of sp^2 bonds, the number of cyclic structures in the three models significantly increases and the structures tend to generate six-membered carbon rings. This is because the six-membered carbon ring has more stable reactivity and higher resistance to stress compared to other rings. As shown in (Figure 2d), the graph statistics of pair distribution functions were analyzed on the structure of three models. The result indicated that the bond growth within the three models was concentrated between 1.42 and 1.55, and there were differences in peak values, which is similar to the research results of Li's paper, verifying the rationality of the internal sp^2 bond content in the model.²⁷ The main parameters of the three models are listed in Table 1. The sp^2 bond contents of the three models were controlled between 40 and 70, with a quantity difference of about 10%.

Table 1. Atomic Percentages of Coke A, Coke B, and Coke C

	Coke A	Coke B	Coke C
carbon atoms	2863	2863	2863
carbon atom ratio	95.4%	95.4%	95.4%
constructed temperature	4000 K	5000 K	6000 K
sp bond contents	15.8%	21.3%	18.7%
sp^2 bond contents	44.8%	57.6%	66.2%
sp^3 bond contents	9.2%	2.6%	1.6%
other bond contents	30.2%	18.5%	13.5%

As shown in Figure 3, the constructed coke model was sliced and some stacked fragments were extracted for comparison. Comparison in terms of structure showed that both models were folded structures composed of multiple carbon rings. This structure has been proven in previous studies to resist external forces by changing the bending angle of the folded layer.³² However, the coke model size in this study is smaller than that in Tian's study, and the structural changes during the reaction process are more significant. In this study, our focus is on studying the effect of the sp^2 bond content on the performance of the model, providing a platform for us to use the model to study the reaction and mechanical properties of coke materials.

3.2. Effect of Different sp^2 Bond Contents on the Reactivity of Coke. To investigate the differences in reaction performance among different models, solution loss reaction simulations were conducted for three models. As shown in Figure 4, the number of carbon atoms in the gasification reaction of three coke models after the reaction in the CO_2 atmosphere, H_2O atmosphere, and mixture atmosphere was statistically analyzed. Compared to the other two models, Coke A has a higher number of carbon atoms in the gasification reaction under three atmospheres, which proved that the lower sp^2 bond content in coke caused a more intense reaction with the oxidation atmosphere. Meanwhile, the results indicated that the

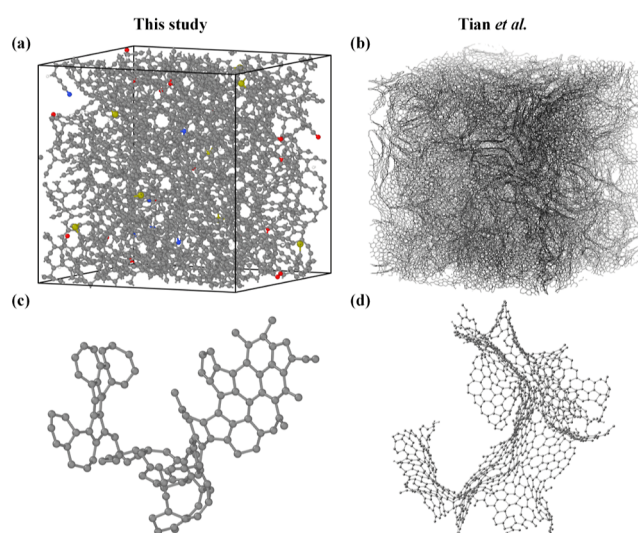


Figure 3. Comparison of the appearance of this study's coke model (a) and Tian's model (b) and comparison of the internal stack structure in this study (c) and in Tian's study (d)³² (Adapted with permission from [Tian, Y.; Li, G.-Y.; Zhang, H.; Wang, J.-P.; Ding, Z.-Z.; Guo, R.; Cheng, H.; Liang, Y.-H., Molecular basis for coke strength: Stacking-fault structure of wrinkled carbon layers. *Carbon* 2020, 162, 56–65.]. Copyright [2020] [Elsevier].).

reactivity of Coke A is more active compared to that of other models with higher sp^2 bond contents, and its structure was more easily corroded under the same atmospheric conditions.

To investigate the differences in reactivity among the three coke models under CO_2 and H_2O atmospheres, the reacted models under a CO_2 atmosphere were analyzed first. The carbon atoms in a CO_2 atmosphere were defined as C_g atoms, and carbon atoms on coke were defined as C atoms. As shown in Figure 5a, from the changes in the reaction curve, the entire process was divided into two stages: stage one is the adsorption process of the CO_2 gas molecules, and stage two is the reaction equilibrium stage. The points of stage transitions are different depending on the structural differences of each model, while they are concentrated in the time of 300–500ps. The red line in the picture is only used to distinguish the areas between the two stages. The specific analysis of stage transition points can be found in the Supporting Information. As shown in Figure 5b, it was observed that activated carbon atoms exist in the internal structure of all three types of coke. This type of carbon atom is more likely to undergo gasification with CO_2 and H_2O , while they mainly exist in a chain-like structure and become the main reaction site for the CO_2 adsorption reaction.²⁹ During the reaction process, free C_gO molecules in the atmosphere would adsorb onto the carbon atoms of the coke, forming suspended CO groups. Subsequently, the C–O bond in the group would break, and C_g atoms would be adsorbed on the surface of the coke while releasing the O atoms. This reaction often occurred on the carbon chain portion or bond-unsaturated carbon atoms in the coke model, while it was difficult for the cyclic carbon structure to undergo such adsorption reactions. Li et al. have also investigated the CO_2 adsorption process of defective graphene.³⁷ In the reaction process, the chain structure generated by defective graphene will capture the CO_2 gas molecules in the atmosphere and make them adsorbed on the vacancy of the graphene, which is similar to the CO_2 adsorption process in stage I. Zhang et al. used DFT to study the adsorption process and reaction process of CO_2 on the surface of defective

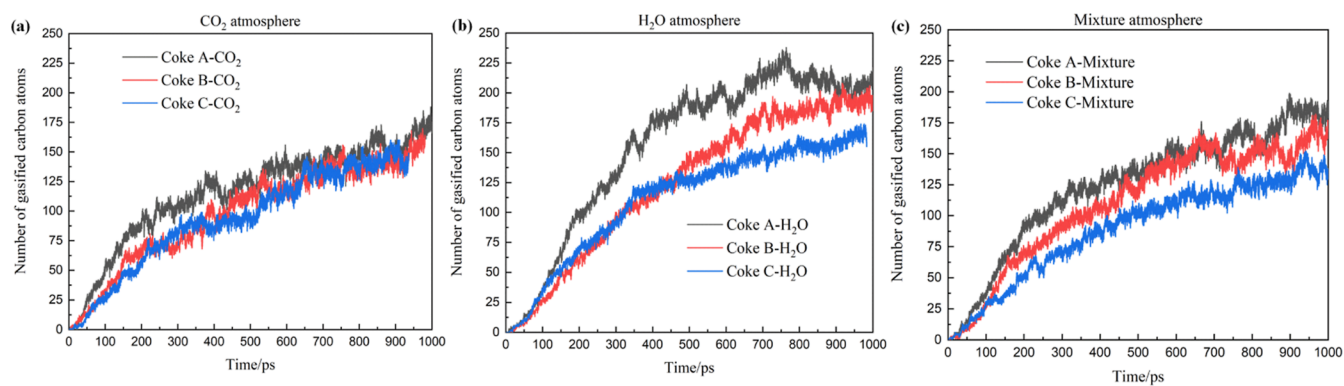


Figure 4. Statistics of the number of gasified carbon atoms under three atmospheres: (a) CO₂ atmosphere; (b) H₂O atmosphere; and (c) mixture atmosphere.

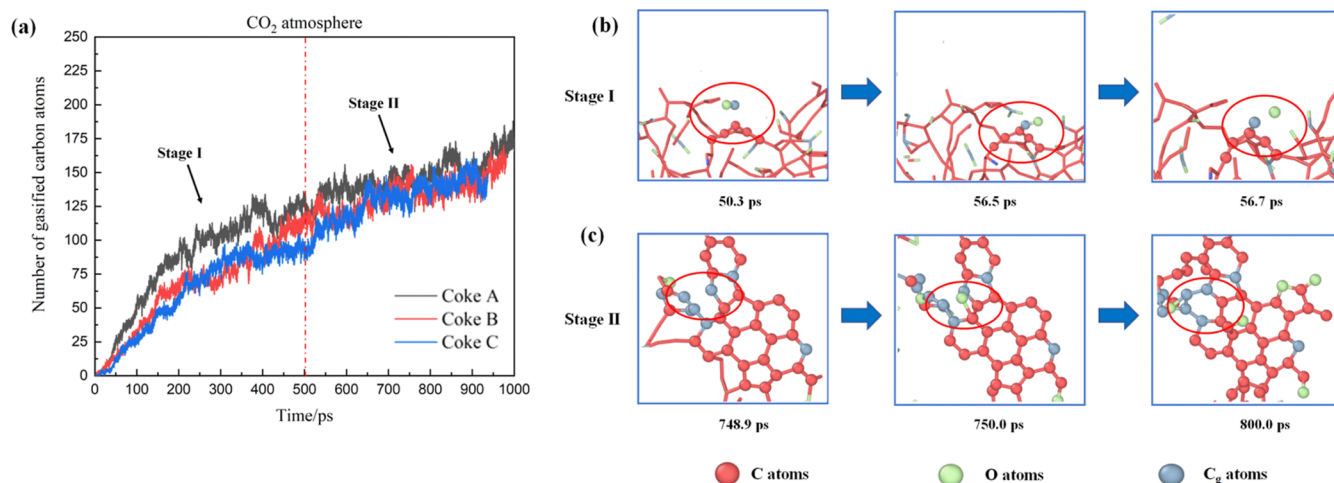


Figure 5. Number of gasified carbon atoms of three types of coke under a CO₂ atmosphere (a) and the relevant mechanism of the gasification process: (b) adsorption process of CO gas and (c) formation process of circular structures.

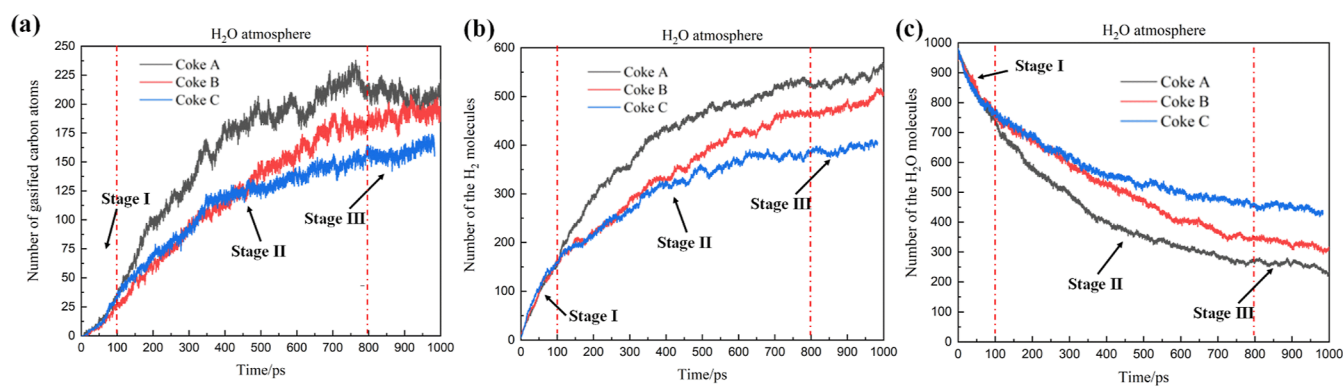


Figure 6. Number of gas molecules in three models under a H₂O atmosphere: (a) number of gasified carbon atoms; (b) H₂ molecular number; and (c) number of H₂O molecules.

graphene, which showed that it is difficult for two CO₂ molecules to adsorb on the same single vacancy.⁴³ The CO₂ adsorption process of a single carbon chain observed in this study is similar to Zhang's research results. Due to the low sp² bond content in Coke A, the number of unsaturated carbon atoms in its structure was significantly higher, allowing for the adsorption of more C_g atoms and gasification reactions during the reaction process. This is also the main reason the number of gasified carbon atoms in Coke A in stage I is significantly higher than those in the other two models.

For stage two of the curve, it was found that the number of carbon atoms in the gasification reaction of the three models remained almost the same and steadily increased. As shown in Figure 5c, it was found that the main reason for this phenomenon was that the adsorbed C_g atoms would generate new C–C bonds with the C atoms on the coke during the reaction process, forming stable ring structures such as five-membered carbon rings and six-membered carbon rings. Compared to the carbon chain structure, the carbon atoms on this circular structure were more stable, and the possibility of

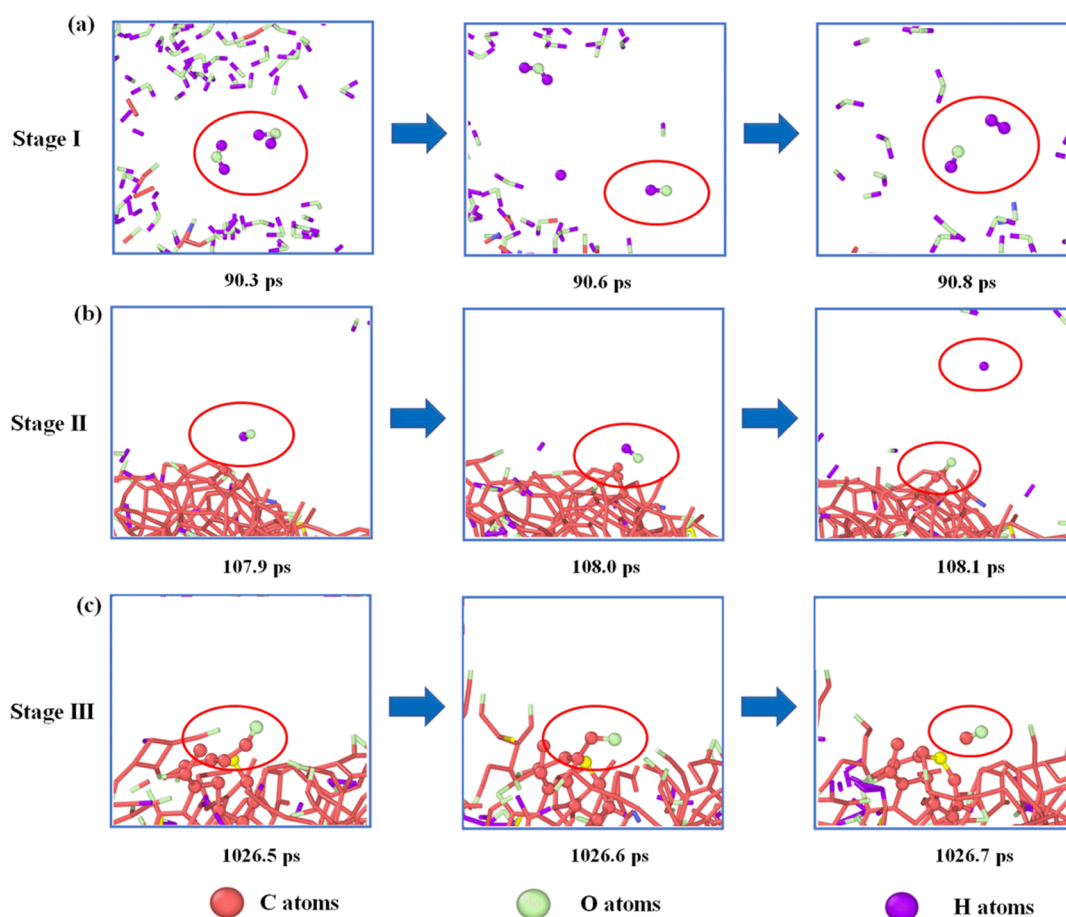


Figure 7. Reaction mechanism of three stages under a H_2O atmosphere: (a) H_2 generation mechanism; (b) $-\text{OH}$ group adsorption mechanism; and (c) CO desorption mechanism.

gasification reactions occurring during the reaction process was lower. After a period of time in the first stage, a similar circular structure was formed on the surface and structure of Coke A, resulting in a decrease in the rate of increase in the number of gasified carbon atoms, which was manifested as the rate of increase in the three curves being basically the same in the second stage.

As shown in Figure 6, statistics were conducted on the number of gasified carbon atoms, H_2 generation, and H_2O molecules in the gasification reaction of three models under a H_2O atmosphere. From the trend of the curve in the figure, the entire reaction process can be divided into three stages: the first stage is the reaction preparation stage. At this stage, the gasification reaction rate, H_2 generation rate, and H_2O molecular consumption rate of the three models are almost equal, and the curves are basically consistent. The reason was that during this stage, the main reaction occurred during the pyrolysis of H_2O molecules at high temperatures, as shown in Figure 7a. Under high-temperature conditions, the $\text{H}-\text{O}$ bond in H_2O molecules would break and detach from the free-state H atom and $-\text{OH}$ group. Subsequently, the H atom would combine with H_2O molecules nearby to generate H_2 molecules and another $-\text{OH}$ group. The first stage was mainly related to the number of H_2O molecules in the atmosphere; therefore, the curve trends of the three models were basically the same. The second stage is the adsorption reaction stage. At this stage, the gasification reaction rate, H_2 generation rate, and H_2O consumption rate of the Coke A curve are significantly higher

than those of the other two models. The reason is that the main reaction occurring in this process was the free-state $-\text{OH}$ adsorption reaction. As shown in Figure 7b, when $-\text{OH}$ groups appeared near the surface of coke, activated carbon atoms with unsaturated carbon chains or bonds undergo adsorption reactions, generating $\text{C}-\text{O}$ bonds to adsorb the free $-\text{OH}$ groups on the surface of coke. Subsequently, the $\text{O}-\text{H}$ bond would break, making the O atom adsorbed on the surface of the coke while detaching from the free H atom. This reaction usually occurs on carbon atoms with unsaturated carbon chains or bonds, and Coke A has the lowest sp^2 bond content, making the gasification reaction rate of this model the fastest, corresponding to a significantly higher number of gasified carbon atoms in Coke A in the second stage curve.

The third stage is the reaction equilibrium stage. During this stage, the curves of the three models gradually tend to be horizontal. Correspondingly, the number of carbon atoms in the gasification reaction of the three models gradually tended to be the same, and the rates of H_2 generation and H_2O molecular consumption tended to be horizontal. The reason is that when a certain number of O atoms were adsorbed on coke, a desorption reaction of CO occurs. The points of stage transitions are different depending on the structural differences of each model, while they are concentrated in the time period of 100–200 and 700–800 ps. The red lines in the picture are only used to distinguish the areas between the two stages. The specific analysis of stage transition points can be found in the Supporting Information. As shown in Figure 7c, as the reaction proceeded,

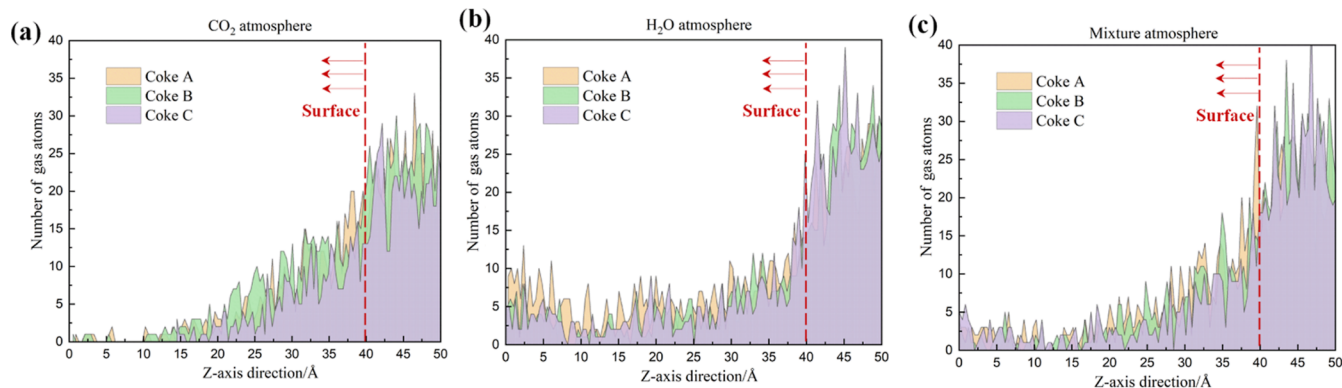


Figure 8. Statistics on the number of gas molecules inside the coke in the different atmospheres: (a) CO₂ atmosphere; (b) H₂O atmosphere; and (c) mixture atmosphere.

the number of atoms adsorbed on the active site of coke reached saturation, leading to the gradual reduction of the generation rate of H₂, accompanied by the reduction of the consumption rate of H₂O molecules. The C atoms adsorbed with O atoms on the surface of coke would undergo C–C bond fracture. At the same time, CO gas would be desorbed and escape from the surface of coke. After the desorption reaction, the active site on the coke surface was vacant again, and the second stage of the adsorption reaction process continued. As the reaction progressed, the reaction rates of the two reactions gradually reached equilibrium, showing a trend toward a horizontal level in the third stage of the curve in Figure 6.

In addition, to investigate the effect of sp² bond content on the permeation rate of gas molecules, statistics were conducted on the number of gas atoms that gas molecules penetrate into the interior of coke. As shown in Figure 8, a statistical analysis was performed on the number of gas atoms penetrating three types of coke in the z-axis direction. The result shows that the adsorption sites of gas molecules in the H₂O atmosphere are deeper than those in the CO₂ atmosphere, indicating that H₂O molecules were more likely to enter the interior of coke for gasification reactions. Compared to the other two types of coke, the number of gas molecules inside coke C is smaller and the distribution area is concentrated on the surface of the coke. This indicates that an increase in the sp² bond content can effectively prevent gas molecules from adsorbing onto the internal structure of the coke and conducting gasification reactions. The reason is that there are more carbon ring structures inside coke C and the ring structure is more stable compared to the carbon chain structure, which reduces the possibility of gasification reactions occurring internally.

3.3. Effect of Different sp² Bond Contents on the Tensile Properties of Coke. The sp² bond not only affects the reactivity of coke but also affects its mechanical properties. This study conducted tensile simulation experiments on the unreacted and reacted models of three types of coke. The direction of stretching is in the y-direction, and the maximum strain is 80%. As shown in Figure 9, the entire stretching process can be divided into three stages. In order to help readers understand the stages better, the stretching curve of Coke A was chosen as the sample curve. Stage one is the elastic stretching process. During this stretching stage, although the coke model undergoes deformation, the stretching deformation is elastic. The stretching stress increases linearly with the increase of strain, and the stress–strain curve shows a straight line with a constant slope. At this point, if the tension is removed, then the

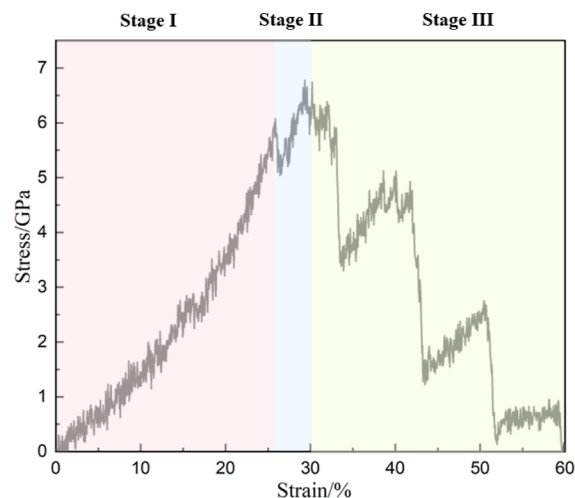


Figure 9. Three stages of the stretching process of model coke A.

coke model can still restore its shape before stretching. The second stage is the plastic stretching stage. The tensile deformation at this stage has become plastic deformation, and the coke has undergone irreversible deformation during the stretching process. The stress–strain curve will still rise and reach the maximum tensile stress value, but the slope of the curve will significantly decrease compared with elastic deformation. At this point, if the pulling force is removed, then the coke cannot return to its original shape. The third stage is the model fracture stage. During this stage of stretching, the coke structure has already broken under the action of tension and the carbon chains connected between each part gradually break. Therefore, even if strain occurs, the stress inside the coke will not increase, manifested as a stepped decrease in the stress curve.

As shown in Figure 10, it was found that the tensile performance of the unreacted model is significantly better than that of the reacted model. The maximum tensile stress of the three types of coke is greater than that of the model after the CO₂/H₂O/mixture atmosphere reaction, indicating that the gas reaction process affects the structure of the coke, leading to a decrease in its tensile resistance. In addition, under the same reaction conditions, the tensile strength of coke C is significantly higher than that of the other two coke models. This proves that with the increase of the sp² bond content, the tensile resistance of coke has been significantly improved and the stability of coke structure has been significantly improved.

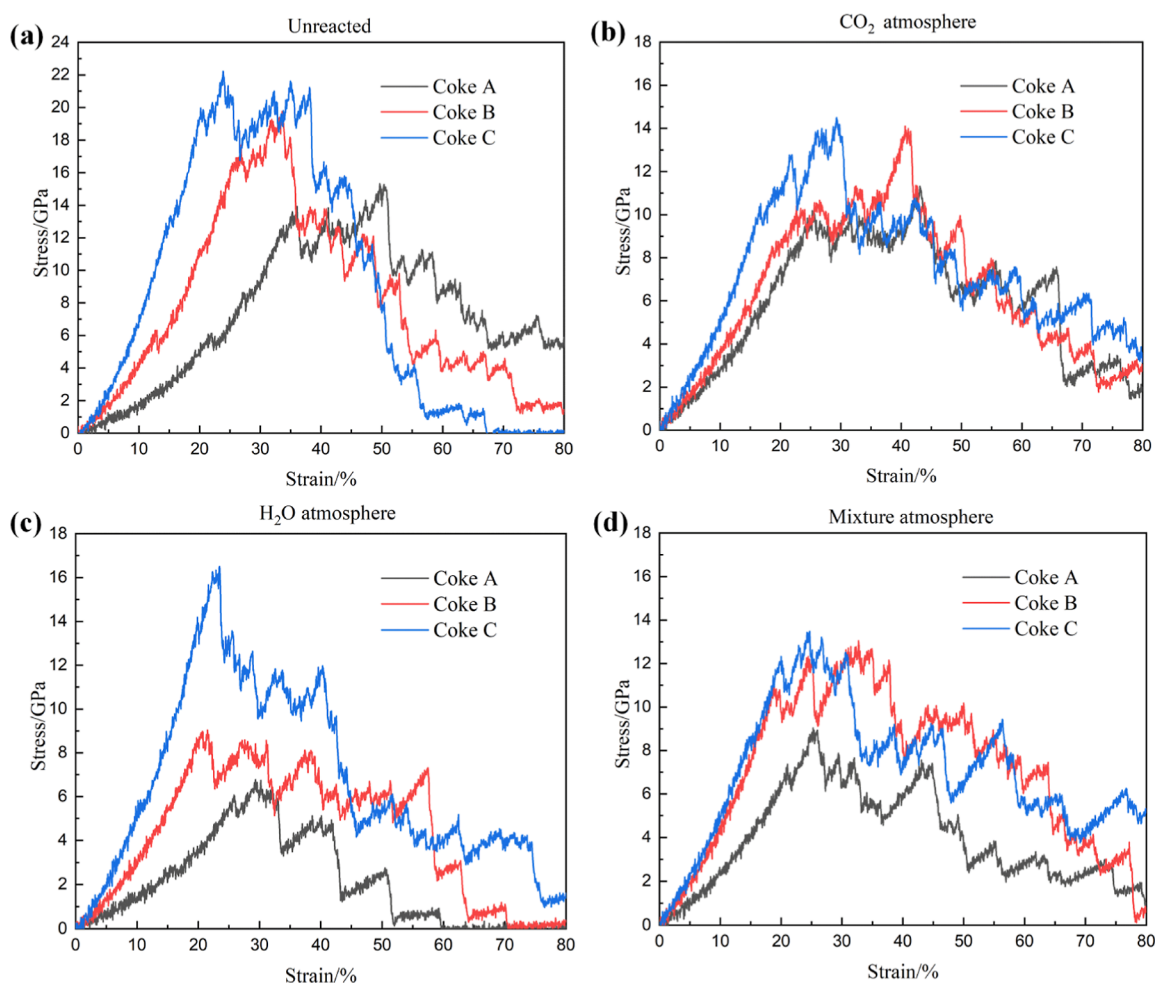


Figure 10. Stress–strain curves of three types of coke models under different conditions: (a) unreacted; (b) CO₂ atmosphere; (c) H₂O atmosphere; and (d) mixture atmosphere.

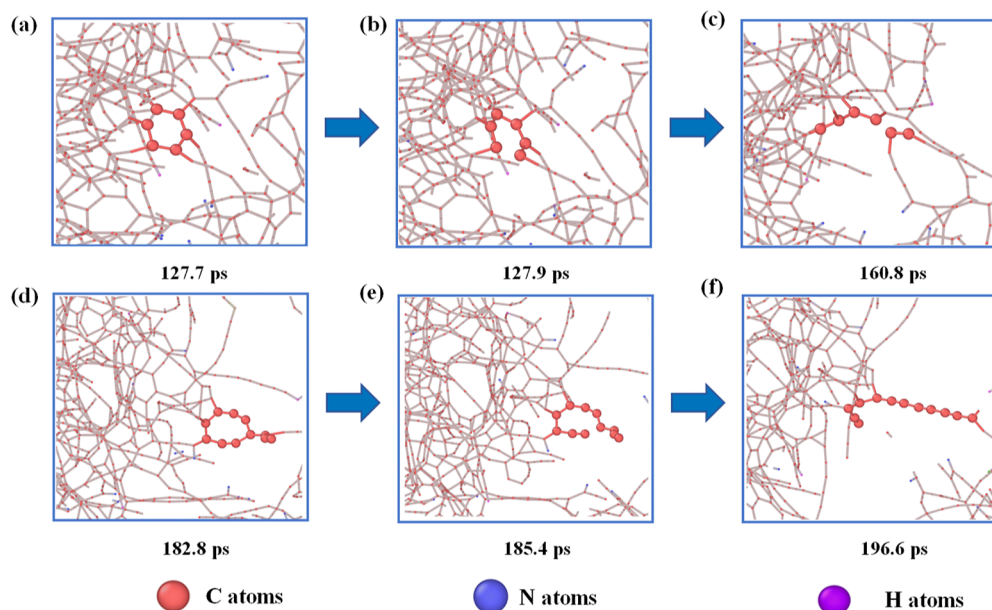


Figure 11. Change mechanism of carbon ring structure during the stretching process: (a–c) six-membered carbon ring change to the carbon chain; (d–f) eight-membered carbon ring change to the carbon chain.

To further investigate the mechanism of the influence of the sp^2 bond on tensile properties, an observation was made on

some fragments during the stretching process. In Tian's previous research, it was pointed out that the chemical bond in the coke

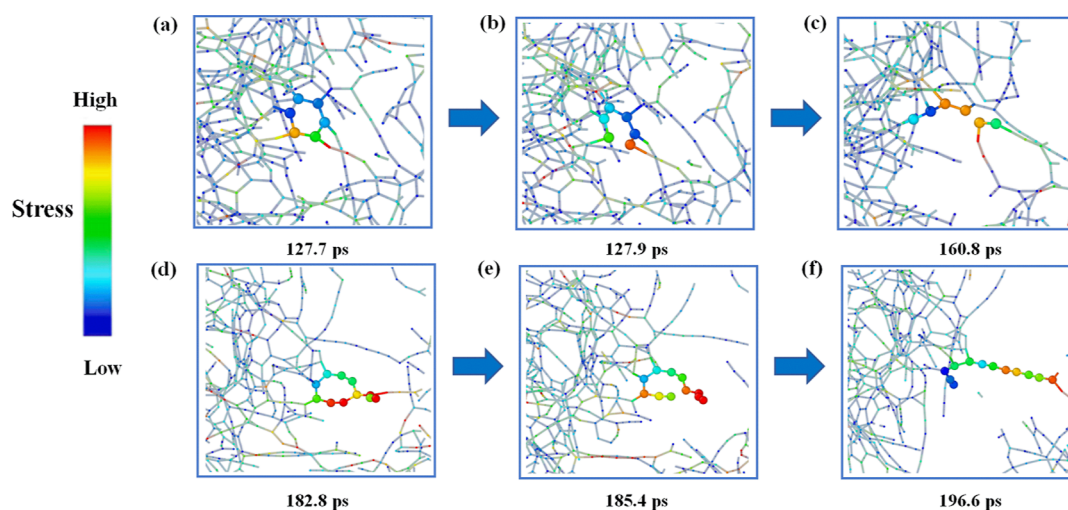


Figure 12. Stress distribution during the structural change of carbon rings: (a–c) six-member carbon ring change to the carbon chain; (d–f) eight-member carbon ring change to the carbon chain.

model can be used to suppress the stack layer translation phenomenon, thus helping to offset the effect of external forces to a certain extent.³² As shown in Figure 11a–c, in addition to the initial carbon chain acting as a resistance to tensile stress, the six-membered carbon ring connected by the sp^2 bond can also inhibit the fracture of the coke model during the stretching process. During the stretching process, the C–C bond in the six-membered carbon ring broke up, and the structure of the six-membered carbon ring transformed into two short carbon chain structures, which were gradually straightened under tensile stress and eventually fractured. During this process, the fracture behavior of the sp^2 bond effectively alleviated the effect of partial strain and evenly distributed the effect of stress, which significantly improved the tensile resistance of coke. In addition, as shown in Figure 11d–f, the C–C bond of the eight-membered carbon ring also broke during stretching, forming a long carbon chain structure with a large number of carbon atoms. However, due to its inferior stability compared to that of the six-membered ring composed of sp^2 bonds, the eight-membered carbon ring had a weaker resistance to tensile stress compared to the six-membered carbon ring.

As shown in Figure 12, a statistical analysis was performed on the stress exerted during the fracture process of the carbon ring mentioned above, and it was plotted into a cloud graph. During the entire stretching process, the atomic forces around the carbon ring were relatively uniform, and there was basically no stress concentration effect. Before the fracture of the carbon ring, a certain carbon atom in the stretching direction on the carbon ring was subjected to a concentrated force, and in the subsequent process, the C–C bond between the atom and adjacent atoms broke. The fracture was accompanied by the disappearance of stress concentration. With the formation of the chain structure, the stress on the carbon chain was evenly distributed to each carbon atom, reducing the concentrated stress on the chemical bond. This effectively improved the maximum stress value at which the carbon chain structure undergoes fracture, thereby significantly enhancing the tensile resistance of the coke model.

4. CONCLUSIONS

In this study, the focus is on the effect of the sp^2 bond content in coke on the reaction performance and mechanical properties of

coke. It has shown that with the decrease of the sp^2 bond content, the reaction performance of coke is significantly reduced. The gasification reaction rate of coke with a higher sp^2 bond content is slower in the dissolution loss reaction. The reason is that compared to other carbon chains inside coke, the six-membered carbon ring structure composed of sp^2 bonds is more stable and the C–C bond is less prone to fracture, making it difficult for –OH groups and CO_2 gas to adsorb on the surface of coke, effectively reducing the gasification reaction rate of coke.

As observed from the tensile simulation experiments, the stretching process of coke was mainly divided into three stages: elastic stretching, plastic stretching, and model fracture. During the stretching process, accompanied by the fracture of the sp^2 bond, the carbon ring structure transforms into multiple short carbon chain structures or a single long carbon chain structure. This phenomenon can effectively reduce the concentration of internal stress in coke, improve the stability of the coke structure during the stretching process, and improve the tensile resistance of coke significantly. The method developed in this article may provide further ideas and platforms for the research on coke performance.

■ ASSOCIATED CONTENT

Supporting Information

The Supporting Information is available free of charge at <https://pubs.acs.org/doi/10.1021/acsomega.3c04411>.

Comparison of gasification of unsaturated bond carbon atoms with another research, calculation results of the absorbed CO_2 molecules and H_2O molecules, details on the specific stage transition points, and calculation results of the sp^2 bond content generated at different temperatures and time steps of coke models (PDF)

Process of six-member carbon ring fracture to resist the tensile stress concentration (MP4)

Process of eight-member carbon ring fracture to resist the tensile stress concentration (MP4)

AUTHOR INFORMATION

Corresponding Author

Kejiang Li – School of Metallurgical and Ecological Engineering, University of Science and Technology Beijing, Beijing 100083, P. R. China; orcid.org/0000-0002-7807-8241; Email: likejiang@ustb.edu.cn

Authors

Zixin Xiong – School of Metallurgical and Ecological Engineering, University of Science and Technology Beijing, Beijing 100083, P. R. China

Yushan Bu – School of Metallurgical and Ecological Engineering, University of Science and Technology Beijing, Beijing 100083, P. R. China

Zeng Liang – School of Metallurgical and Ecological Engineering, University of Science and Technology Beijing, Beijing 100083, P. R. China

Hang Zhang – Modern Technology and Education Centre, North China University of Science and Technology, Tangshan 063009, Tangshan, PR China

Haotian Liao – School of Metallurgical and Ecological Engineering, University of Science and Technology Beijing, Beijing 100083, P. R. China

Feng Zhou – School of Metallurgical and Ecological Engineering, University of Science and Technology Beijing, Beijing 100083, P. R. China

Jianliang Zhang – School of Metallurgical and Ecological Engineering, University of Science and Technology Beijing, Beijing 100083, P. R. China

Complete contact information is available at:

<https://pubs.acs.org/10.1021/acsomega.3c04411>

Author Contributions

Z.X.: validation, investigation, data curation, and writing—original draft. K.L.: conceptualization, writing—review and editing, and supervision. Y.B.: visualization and conceptualization. Z.L.: methodology. H.Z.: software. H.L.: conceptualization. F.Z.: methodology. J.Z.: supervision.

Notes

The authors declare no competing financial interest.

ACKNOWLEDGMENTS

The authors acknowledge the financial support from the Young Elite Scientist Sponsorship Program by CAST (YESS20210090), the National Natural Science Foundation of China (51974019 and 51804025), and the National Key Research and Development Program of China (2017YFB0304300 and 2017YFB0304303).

REFERENCES

(1) Xu, R.; Dai, B.; Wang, W.; Schenk, J.; Bhattacharyya, A.; Xue, Z. Gasification Reactivity and Structure Evolution of Metallurgical Coke under H₂O/CO₂ Atmosphere. *Energy Fuels* **2018**, *32* (2), 1188–1195.

(2) Hasanbeigi, A.; Arens, M.; Price, L. Alternative emerging ironmaking technologies for energy-efficiency and carbon dioxide emissions reduction: A technical review. *Renew. Sustain. Energy Rev.* **2014**, *33*, 645–658.

(3) Zhong, Q.; Mao, Q.; Zhang, L.; Xiang, J.; Xiao, J.; Mathews, J. P. Structural features of Qingdao petroleum coke from HRTEM lattice fringes: Distributions of length, orientation, stacking, curvature, and a large-scale image-guided 3D atomistic representation. *Carbon* **2018**, *129*, 790–802.

(4) Sun, M.; Zhang, J.; Li, K.; Barati, M.; Liu, Z. Co-gasification characteristics of coke blended with hydro-char and pyro-char from bamboo. *Energy* **2022**, *241*, 122890.

(5) Dastidar, M. G.; Bhattacharyya, A.; Sarkar, B. K.; Dey, R.; Mitra, M. K.; Schenk, J. The effect of alkali on the reaction kinetics and strength of blast furnace coke. *Fuel* **2020**, *268*, 117388.

(6) Huang, J.; Guo, R.; Wang, Q.; Liu, Z.; Zhang, S.; Sun, J. Coke solution-loss degradation model with non-equimolar diffusion and changing local pore structure. *Fuel* **2020**, *263*, 116694.

(7) Wang, Q.; Guo, R.; Zhao, X.-f.; Sun, J.-f.; Zhang, S.; Liu, W.-z. A new testing and evaluating method of cokes with greatly varied CRI and CSR. *Fuel* **2016**, *182*, 879–885.

(8) Li, K.; Khanna, R.; Zhang, J.; Liu, Z.; Sahajwalla, V.; Yang, T.; Kong, D. The evolution of structural order, microstructure and mineral matter of metallurgical coke in a blast furnace: A review. *Fuel* **2014**, *133*, 194–215.

(9) Zhang, X.; Zhang, J.; Guo, R.; Xiao, Q.; Feng, Y.; Cheng, H. Highly reactive coke made from Low-rank Coal: Relationship between thermal properties and multilevel structure. *Fuel* **2023**, *337*, 127186.

(10) Pang, K.; Meng, X.; Zheng, Y.; Liu, F.; Wan, C.; Gu, Z.; Sun, M.; Wu, H. Effect of gasification reaction on pore structure, microstructure, and macroscopic properties of blast furnace coke. *Fuel* **2023**, *350*, 128694.

(11) Chang, Z.-y.; Wang, P.; Zhang, J.-l.; Jiao, K.-x.; Zhang, Y.-q.; Liu, Z.-j. Effect of CO₂ and H₂O on gasification dissolution and deep reaction of coke. *Int. J. Miner. Metall. Mater.* **2018**, *25* (12), 1402–1411.

(12) Xu, J.; Zuo, H.; Wang, G.; Zhang, J.; Guo, K.; Liang, W. Gasification mechanism and kinetics analysis of coke using distributed activation energy model (DAEM). *Appl. Therm. Eng.* **2019**, *152*, 605–614.

(13) Xu, Y.; Gao, F.; Ren, H.; Zhang, Z.; Jiang, X. An Iterative Distortion Compensation Algorithm for Camera Calibration Based on Phase Target. *Sensors* **2017**, *17* (6), 1188.

(14) Sun, M.; Zhang, J.; Li, K.; Wang, Z.; Jiang, C.; Li, H. Negatively Catalyzed Gasification Characteristics of Metallurgical Coke and its Implication for Ironmaking Process. *ISIJ Int.* **2021**, *61* (3), 674–683.

(15) Gouws, S. M.; Neomagus, H. W. J. P.; Roberts, D. G.; Bunt, J. R.; Everson, R. C. The effect of carbon dioxide partial pressure on the gasification rate and pore development of Highveld coal chars at elevated pressures. *Fuel Process. Technol.* **2018**, *179*, 1–9.

(16) Meng, F.; Shao, L.; Zou, Z. Investigation of the Effects of Coke Reactivity and Iron Ore Reducibility on the Gas Utilization Efficiency of Blast Furnace. *Energies* **2020**, *13* (19), 5062.

(17) Porada, S.; Czerski, G.; Grzywacz, P.; Makowska, D.; Dziok, T. Comparison of the gasification of coals and their chars with CO₂ based on the formation kinetics of gaseous products. *Thermochim. Acta* **2017**, *653*, 97–105.

(18) Zhu, H.-b.; Zhan, W.-l.; He, Z.-j.; Yu, Y.-c.; Pang, Q.-h.; Zhang, J.-h. Pore structure evolution during the coke graphitization process in a blast furnace. *Int. J. Miner. Metall. Mater.* **2020**, *27* (9), 1226–1233.

(19) Hamada, T.; Suzuki, K.; Kohno, T.; Sugiura, T. Structure of coke powder heat-treated with boron. *Carbon* **2002**, *40* (8), 1203–1210.

(20) Wang, Y.; Dong, Y. W.; Zhong, C. G.; Cao, Q. The effect of mechanical vibration on the structure of needle coke prepared from a modified coal tar pitch. *New Carbon Mater.* **2017**, *32* (5), 467–473.

(21) Sun, M.; Zhang, J.; Li, K.; Guo, K.; Wang, H.; Wang, Z.; Jiang, C. Influence of Structure and Mineral Association of Tuyere-Level Coke on Gasification Process. *Metall. Mater. Trans. B* **2018**, *49* (5), 2611–2621.

(22) Zhang, H.; Bai, J.; Li, W.; Cheng, F. Comprehensive evaluation of inherent mineral composition and carbon structure parameters on CO₂ reactivity of metallurgical coke. *Fuel* **2019**, *235*, 647–657.

(23) Xiong, Z.; Syed-Hassan, S. S. A.; Xu, J.; Wang, Y.; Hu, S.; Su, S.; Zhang, S.; Xiang, J. Evolution of coke structures during the pyrolysis of bio-oil at various temperatures and heating rates. *J. Anal. Appl. Pyrolysis* **2018**, *134*, 336–342.

(24) Lu, Y.; Kocaefe, D.; Kocaefe, Y.; Huang, X.-A.; Bhattacharyya, D. The wettability of coke by pitches with different quinoline-insoluble contents. *Fuel* **2017**, *199*, 587–597.

- (25) Sato, H.; Aoki, H.; Miura, T.; Patrick, J. W. Estimation of thermal stress in lump coke. *Fuel* **1997**, *76* (4), 303–310.
- (26) Zi-Zhao, D.; Zhang, S.; Qiang, L.; Ming-Hui, D.; Rui, G.; Jie-Ping, W.; Guang-Yue, L.; Ying-Hua, L. Boudouard reaction accompanied by graphitization of wrinkled carbon layers in coke gasification: A theoretical insight into the classical understanding. *Fuel* **2021**, *297*, 120747.
- (27) Li, K.; Zhang, H.; Li, G.; Zhang, J.; Bouhadja, M.; Liu, Z.; Skelton, A. A.; Barati, M. ReaxFF Molecular Dynamics Simulation for the Graphitization of Amorphous Carbon: A Parametric Study. *J. Chem. Theory Comput.* **2018**, *14* (5), 2322–2331.
- (28) Liang, Z.; Khanna, R.; Li, K.; Guo, F.; Ma, Y.; Zhang, H.; Bu, Y.; Bi, Z.; Zhang, J. Impact of oxidants O₂, H₂O, and CO₂ on graphene oxidation: A critical comparison of reaction kinetics and gasification behavior. *Chem. Eng. J.* **2022**, *450*, 138045.
- (29) Xiong, Z.; Liang, Z.; Bu, Y.; Li, K.; Zhang, H.; Zhang, J. The effect of vacancy size on the oxidation process of graphene by CO₂: A ReaxFF molecular dynamics study. *Diamond Relat. Mater.* **2023**, *136*, 109989.
- (30) Bu, Y.; Li, K.; Guo, F.; Liang, Z.; Zhang, J. Mechanical behavior and failure mechanism of multilayer graphene oxides with various oxygen contents and functional types: A ReaxFF molecular dynamics simulation. *Appl. Surf. Sci.* **2022**, *606*, 154920.
- (31) Liang, Z.; Li, K.; Guo, F.; Zhang, H.; Bu, Y.; Zhang, J. The Dynamic Nature of Graphene Active Sites in the H₂O Gasification process: A ReaxFF and DFT Study. *J. Mol. Model.* **2023**, *29* (4), 116.
- (32) Tian, Y.; Li, G.-Y.; Zhang, H.; Wang, J.-P.; Ding, Z.-Z.; Guo, R.; Cheng, H.; Liang, Y.-H. Molecular basis for coke strength: Stacking-fault structure of wrinkled carbon layers. *Carbon* **2020**, *162*, 56–65.
- (33) Lu, Q.; Guo, R.; Zhang, H.; Wang, J.-P.; Lu, T.; Li, G.-Y.; Liang, Y.-H. To stimulate, and to inhibit: A theoretical understanding of the sodium-catalytic mechanism of coke gasification. *Chem. Eng. J.* **2022**, *435*, 135091.
- (34) Plimpton, S. Fast Parallel Algorithms for Short-Range Molecular Dynamics. *J. Comput. Phys.* **1995**, *117* (1), 1–19.
- (35) Chenoweth, K.; van Duin, A. C. T.; Goddard, W. A. ReaxFF Reactive Force Field for Molecular Dynamics Simulations of Hydrocarbon Oxidation. *J. Phys. Chem. A* **2008**, *112* (5), 1040–1053.
- (36) van Duin, A. C. T.; Dasgupta, S.; Lorant, F.; Goddard, W. A. ReaxFF: A Reactive Force Field for Hydrocarbons. *J. Phys. Chem. A* **2001**, *105* (41), 9396–9409.
- (37) Li, K.; Khanna, R.; Zhang, H.; Ma, S.; Liang, Z.; Li, G.; Barati, M.; Zhang, J. Thermal behaviour during initial stages of graphene oxidation: Implications for reaction kinetics and mechanisms. *Chem. Eng. J.* **2021**, *421*, 129742.
- (38) Li, K.; Li, H.; Sun, M.; Zhang, J.; Zhang, H.; Ren, S.; Barati, M. Atomic-Scale Understanding about Coke Carbon Structural Evolution by Experimental Characterization and ReaxFF Molecular Dynamics. *Energy Fuels* **2019**, *33* (11), 10941–10952.
- (39) Kumar, R.; Parashar, A. Dislocation assisted crack healing in h-BN nanosheets. *Phys. Chem. Chem. Phys.* **2017**, *19* (32), 21739–21747.
- (40) Verma, A.; Parashar, A. Molecular dynamics based simulations to study the fracture strength of monolayer graphene oxide. *Nanotechnology* **2018**, *29* (11), 115706.
- (41) Zhao, H.; Min, K.; Aluru, N. R. Size and Chirality Dependent Elastic Properties of Graphene Nanoribbons under Uniaxial Tension. *Nano Lett.* **2009**, *9* (8), 3012–3015.
- (42) Vimal, M.; Sandfeld, S.; Prakash, A. Grain segmentation in atomistic simulations using orientation-based iterative self-organizing data analysis. *Materialia* **2022**, *21*, 101314.
- (43) Zhang, S.; Liang, Z.; Li, K.; Zhang, J.; Ren, S. A density functional theory study on the adsorption reaction mechanism of double CO₂ on the surface of graphene defects. *J. Mol. Model.* **2022**, *28* (5), 118.